APPLIED AND ENVIRONMENTAL MICROBIOLOGY, July 2001, p. 3188–3194 Vol. 67, No. 7
0099-2240/01/$04.00+0 DOI: 10.1128/AEM.67.7.3188–3194.2001

Adhesion of *Pseudomonas fluorescens* (ATCC 17552) to Nonpolarized and Polarized Thin Films of Gold

J. P. BUSALMEN* AND S. R. DE SÁNCHEZ

División Corrosión, INTEMA-CONICET, Universidad Nacional de Mar del Plata, B7608FDQ Mar del Plata, Argentina

Received 8 January 2001/Accepted 16 April 2001

The adhesion of *Pseudomonas fluorescens* (ATCC 17552) to nonpolarized and negatively polarized thin films of gold was studied in situ by contrast microscopy using a thin-film electrochemical flow cell. The influence of the electrochemical potential was evaluated at two different ionic strengths (0.01 and 0.1 M NaCl; pH 7) under controlled flow. Adhesion to nonpolarized gold surfaces readily increased with the time of exposition at both ionic-strength values. At negative potentials (−0.2 and −0.5 V [Ag/AgCl-KCl saturated {sat.}]), on the other hand, bacterial adhesion was strongly inhibited. At 0.01 M NaCl, the inhibition was almost total at both negative potentials, whereas at 0.1 M NaCl the inhibition was proportional to the magnitude of the potential, being almost total at −0.5 V. The existence of reversible adhesion was investigated by carrying out experiments under stagnant conditions. Reversible adhesion was observed only at potential values very close to the potential of zero charge of the gold surface (0.0 V [Ag/AgCl-KCl sat.]) at a high ionic strength (0.1 M NaCl). Theoretical calculations of the Derjaguin-Landau-Verwey-Overbeek (DLVO) interaction energy for the bacteria-gold interaction were in good agreement with experimental results at low ionic strength (0.01 M). At high ionic strength (0.1 M), deviations from DLVO behavior related to the participation of specific interactions were observed, when surfaces were polarized to negative potentials.

Adhesion of bacteria to solid surfaces is a general phenomenon associated with numerous medical, industrial, and ecological problems (4, 7, 8, 11, 19, 22). In particular, the adhesion to metal surfaces is related, for example, to the contamination of prosthetic and medical devices (7) or to the localized corrosion failure of industrial equipment (4), as a consequence of the bacterial surface colonization and biofilm formation. A better understanding of the variables governing bacterial adhesion to metal surfaces will surely contribute to funding solutions to these problems.

The interaction between bacterial cells and solid surfaces is often described by the Derjaguin-Landau-Verwey-Overbeek (DLVO) theory of colloid stability, developed by Derjaguin and Landau in 1941 and Verwey and Overbeek in 1947 (14). This theory summarizes the electrostatic and van der Waals interactions, yielding the overall interaction energy between surfaces as a function of separation distance. In addition to these nonspecific interactions, specific interactions have been described participating in the bacterial adhesion process, including the formation of ionic, hydrogen, and chemical bonds (3).

It was been pointed out that a reliable study of bacterial adhesion requires well-defined hydrodynamic conditions and must prevent alteration of results by avoiding the passage of samples through the air-liquid interface (15, 16). These experimental constrains have been often circumvented while studying the adhesion of bacteria to glass using both flow cell systems with well-defined flow conditions and an in situ technique for the observation of the interface (13). Following the same strategies, in the present work we developed an experimental system which allows the in situ observation of bacterial adhesion to metal surfaces by phase-contrast microscopy and under controlled flow conditions. Furthermore, since the system includes the possibility of an electrochemical control over the metal surface, we studied the influence of electrochemical variables on bacterial adhesion.

The objective of this work was to evaluate the influence of the electrochemical potential on the bacterial adhesion to metals. Gold was selected for the experiments as a model surface because it is a widely studied noble metal and most of its physicochemical constants are available in the literature (1, 20). In addition, the gold surface composition remains constant over a wide potential interval, and only changes of the electrostatic surface charge due to the capacitive behavior of the electrical double layer take place (18).

In this work, the existence of both reversible and irreversible adhesion was demonstrated. Experimental results were compared with DLVO calculations of the interaction energy at various potential and ionic strength values.

MATERIALS AND METHODS

Biological material. Pure cultures of *Pseudomonas fluorescens* (ATCC 17552) were grown at 32°C with continuous shaking in a rich broth containing Lab Lemco (Merck) (0.1 g liter^{-1}), yeast extract (Sigma) (0.2 g liter^{-1}), and peptone (Sigma) (0.5 g l^{-1}) dissolved in 0.1 M NaCl, pH 7. Cells were harvested from cultures at the exponential phase of growth by centrifugation for 10 min at 10,000 × *g* in a Jouan BR4i refrigerated centrifuge, washed with 0.1 M NaCl (pH 7), and suspended in NaCl solutions of different ionic strengths (0.01 and 0.1 M NaCl, pH 7) after being centrifuged again.

Electrophoretic mobility. The zeta potential (ζ) of bacterial cells suspended in NaCl solutions (0.01 and 0.1 M) at a final cell number of 10^5 cells ml^{-1}, was determined by electrophoretic migration. A Rank Bros., Ltd., Mark II particle microelectrophoresis apparatus (Bottisham, Cambridge, England) was used. The applied potential was 80 V. The value of ζ was calculated using Smoluchowski's equation as $\zeta = 12.87\ \mu$ (5), where μ is the measured electrophoretic migration.

* Corresponding author. Mailing address: División Corrosión-INTEMA, UNMdP, Juan B. Justo 4302, B7608FDQ Mar del Plata, Argentina. Phone: 54 223 4816600. Fax: 54 223 4810046. E-mail: jbusalme@fi.mdp.edu.ar.

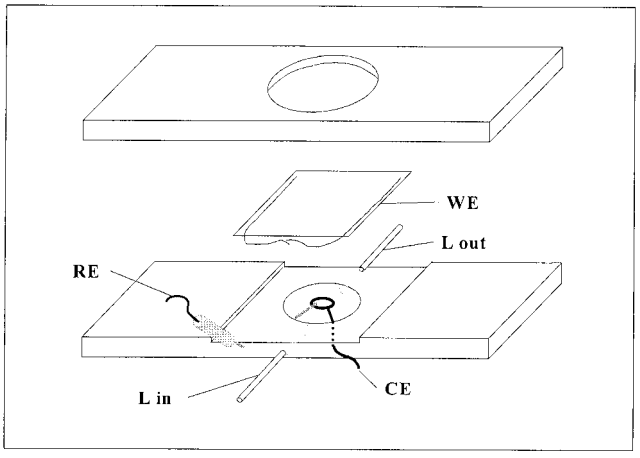

FIG. 1. Schematic diagram of the thin film electrochemical flow cell designed for microscopic observations. Bacterial suspension is pumped into the chamber through stainless steel liquid inlets (L in and L out) at a controlled flow. The thin-film gold WE is placed facing down and microscopic observations are made from the back. A platinum wire CE circumvents the light path on the bottom of the chamber to ensure a uniform current distribution. The reference electrode (RE) is connected through a salt bridge to improve conductivity.

Electrochemical thin-film flow cell. A thin-film electrochemical flow cell was especially designed for observation with an optical microscope. A schematic representation of the cell is shown in Fig. 1. It was constructed from a 75- by 35- by 3-mm acrylic piece and contained a shallow (2-mm) central chamber of 14 mm in diameter, through which the bacterial suspension was pumped. The working electrode (WE) was used as a lid for the chamber. It was constructed by sputtering a thin film (10 to 20 nm) of gold onto a glass coverslip. The coverslip was previously degreased with chloroform, cleaned by immersion in chromic acid, and washed gently with double-distilled water and ethanol. The integrity of gold films was verified by microscopic observation and their electric resistance was measured in order to ensure electric conductivity.

The thin-film electrode was placed facing down on the chamber, sealed with silicone grease, and secured with an O-ring with an acrylic lid screwed at both sides of the cell body. The electrical contact for the WE was established by means of two 0.2-μm copper wires placed at both sides of the chamber, on the unexposed electrode area. The counter electrode (CE) was a 0.75-mm platinum wire loop which was placed on the bottom of the chamber, circumventing the light path, to ensure an uniform current distribution throughout the working observation area. The Luggin for the reference electrode was a salt bridge constructed with a stainless steel syringe needle filled with 1% agar in a 1% NaCl solution. This procedure improves the electric conductivity and ensures an appropriate reading of the reference potential.

The thin-film WE allows the observation of adhered bacteria from the back side. Observations were done by phase contrast with an Olympus BH transmission microscope equipped with a 100×, 1.3 numerical aperture oil immersion phase-contrast lens, an IF550 green filter, and a phase-contrast condenser. Images were captured with a charge-coupled device camera and recorded on VHS tapes with a conventional video recorder.

The cell was connected through stainless steel inlets with a silicone rubber tubing flow system. Experiments were done under a flow of 0.7 ml min^{-1}, controlled by a low-flow peristaltic pump. A pulse dampener was used to avoid pulsation in the liquid.

Adhesion measurements. Once the cell was assembled and filled with NaCl solution, the working electrode was polarized at the desired potential using an EG&G 362 scanning potentiostat (Princeton Applied Research, Princeton, N.J.). An Ag/AgCl-KCl saturated (sat.) electrode was taken as the reference. Measurements were done at potentials of −0.5 and −0.2 V, at the open circuit potential (E_{oc}= 0.2 V) (Ag/AgCl-KCl sat.), and at two different ionic strength values, 0.01 and 0.1 M NaCl.

The bacterial suspension containing 2×10^8 to 3×10^8 cells ml^{-1} was pumped into the chamber, and cell adhesion to the working electrode was recorded on video tape during 15 min. Sequential gray-scale images were captured from the video tapes at 30-s time intervals to determine the kinetics of bacterial adhesion under the different experimental conditions.

The digital analysis of images was done with the public domain NIH Image software, developed at the National Institute of Health, which can be obtained from http://rsb.nih.info.gov/nih.image/.

Every image was divided by the previous one and multiplied by 255 in order to obtain, time to time, a resulting image containing only the newly adhered bacteria. Out-of-focus moving bacterial cells were clearly distinguished and ignored during the analysis process. Using this process, newly attached cells appear as black (gray value, 255) spots on the background color. On the other side, detachment can be recognized by the appearance of white (gray value, 0) spots.

To determine the occurrence of reversible adhesion, additional measurements were carried out under stagnant conditions, at the same surface potentials previously used (−0.5 V, −0.2 V and E_{oc} [Ag/AgCl-KCl sat.]). An additional surface potential value of 0.00 V (Ag/AgCl-KCl sat.) was also included. In these experiments, the bacterial suspension was manually injected with a disposable syringe. Stagnant conditions were chosen in order to improve the observation of bacterial movements in association with the surface without interference from bacteria moving by the action of flow.

Sequential images were captured from the video records at a rate of 12 images s^{-1} and analyzed with the NIH Image software as follows.

Images (n_i) were subtracted with the previous one (n_{i-1}) to obtain differential displacement images [$d(t)$] of moving bacteria with 1/12-s time intervals. These subtractions yielded differential images in which, beside the bacteria in their present position at n_{i-1}, the position of the bacteria at n_i appears as white footprints. Differential images [$d(t = 1/12)$, $d(t = 2/12) \ldots d(t = n/12)$] were compiled, and the minimal gray value for every pixel during a 5-s (60/12-s) time period was selected. This selection yielded a new image containing the (white) footprints of moving bacteria at every time interval. The resulting image was multiplied by the last differential image [$d(t = 60/12)$] to include bacteria at their present position in the result of the analysis.

Calculations of interaction forces between bacteria and gold surfaces. The interaction energies [$G_{DLVO}(h)$] between the bacterial surfaces and the gold surfaces were calculated according to the DLVO theory of colloidal stability with the mathematical equations in reference 14. $G_{DLVO}(h)$ is the energy resulting from the sum of van der Waals and electrostatic interactions. The van der Waals attraction is proportional to the Hamaker constant for the interaction between bacteria and gold across water [$A_{bg(w)}$] and was calculated from the values of the Hamaker constants for each material (14):

$$A_{bg(w)} = (A_g^{1/2} - A_w^{1/2}) - (A_b^{1/2} - A_w^{1/2}) \quad (1)$$

where A_g, A_b, and A_w are the Hamaker constants for the gold surface, the bacterial surfaces, and the surrounding water, respectively.

Electrostatic interactions depend on the electrical potentials of the surfaces. The potential of the metallic surface was externally controlled and the values relative to its potential of zero charge (PZC) were used in the calculations. In the case of the bacterial surfaces, the electrokinetic or zeta potential (ζ) was used instead of the electric potential, with the assumptions that the bacterial surface is flat and that the charge is located on the plane of shear (5, 21). However, it should be noted that the distance h between a flat gold surface and the plane of shear of a bacterial cell is a very approximate value.

RESULTS

Adhesion of *P. fluorescens* (ATCC 17552) to nonpolarized and polarized gold at 0.01 M NaCl. To determine the kinetics of bacterial adhesion to gold without any external modification of the surface electrochemistry, experiments were performed using bacterial suspensions in 0.01 M NaCl and with the gold surface at its open circuit potential (E_{oc}= 0.2 ± 0.02 V [Ag/AgCl-KCl sat.]). Results can be observed in Fig. 2. The number of adhered bacteria readily increased with the time of exposition to the flowing bacterial suspension, reaching 4.5×10^4 bacteria mm^{-2} after 15 min. Under these experimental conditions, the spontaneous and irreversible adhesion of all the cells reaching the surface was observed. When the surface potential was externally controlled at a negative value, a strong inhibition of the bacterial adhesion kinetics was observed. Both at −0.2 and −0.5 V (Ag/AgCl-KCl sat.), the number of adhered

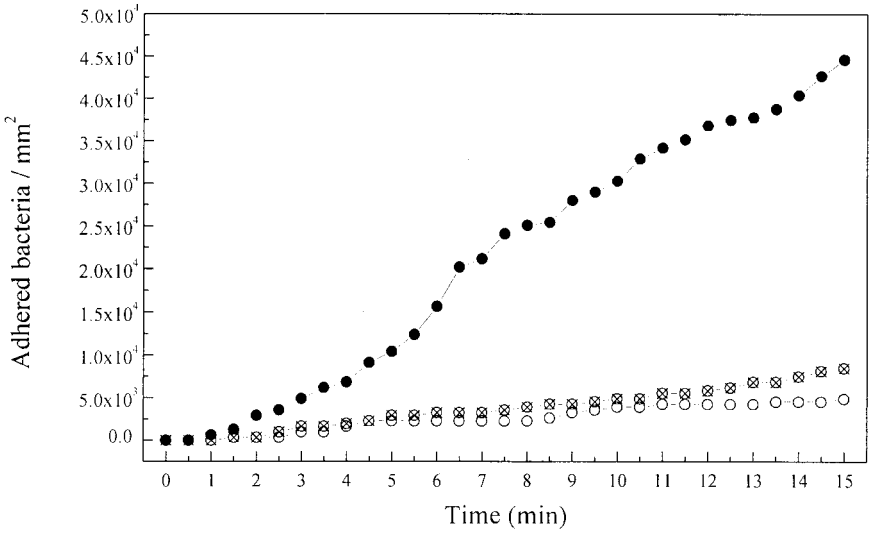

FIG. 2. Variations of the number of adhered bacteria to the gold surface at various surface potentials, with the time of exposition to a flowing bacterial suspension in 0.01 M NaCl, pH 7. ●, 0.2 V (E_{oc}); ⊗, −0.2 V; ○, −0.5 V. An Ag/AgCl-KCl sat. electrode was taken as a reference. The flow rate was 0.7 ml min^{-1}.

bacteria was extremely low, 0.75×10^4 and 0.4×10^4 bacteria mm $^{-2}$, respectively, compared to the one obtained at the E_{oc} (Fig. 2).

Adhesion of *P. fluorescens* (ATCC 17552) to nonpolarized and polarized gold at 0.1 M NaCl. The effect of increasing the ionic strength on the electrochemical potential influence on bacterial adhesion was investigated. The experiments described above were repeated, using in this case bacterial suspensions in 0.1 M NaCl solution. The results are shown in Fig. 3. The higher number of adhered bacteria was observed once again with the metallic surface at the E_{oc}. After 15 min of exposition, about 2.5×10^4 bacteria mm^{-2} were adhered. This number was relatively lower than the one obtained at 0.01 M (4.5×10^4 bacteria mm^{-2}) (Fig. 2).

On the other hand, when the experiments were carried out at a potential of −0.2 V (Ag/AgCl-KCl sat.), about 1.5×10^4 bacteria mm^{-2} were adhered (Fig. 3), this number being relatively higher than the one observed at 0.01 M NaCl (0.75×10^4 bacteria mm^{-2}) (Fig. 2). The bacterial adhesion at −0.5 V (Ag/AgCl-KCl sat.) was negligible (Fig. 3), as in the previous experiments under this condition (Fig. 2).

Calculations of the DLVO interaction energy curves. Interaction energy curves were calculated for the DLVO interactions between gold and bacteria in water. Values of 62.5 kT (1),

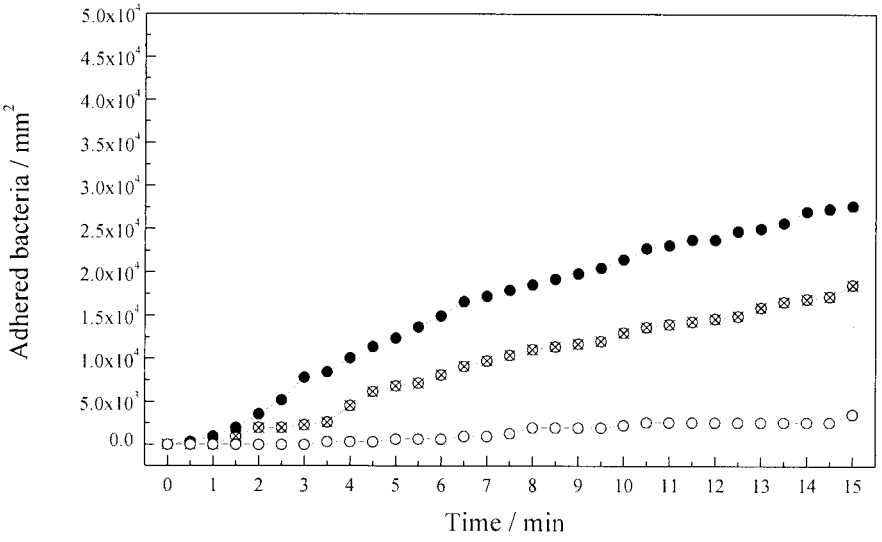

FIG. 3. Variations of the number of adhered bacteria to the gold surface at various surface potentials, with the time of exposition to a flowing bacterial suspension in 0.1 M NaCl, pH 7. ●, 0.2 V (E_{oc}); ⊗, −0.2 V; ○, −0.5 V. An Ag/AgCl-KCl sat. electrode was taken as a reference. The flow rate was 0.7 ml min^{-1}.

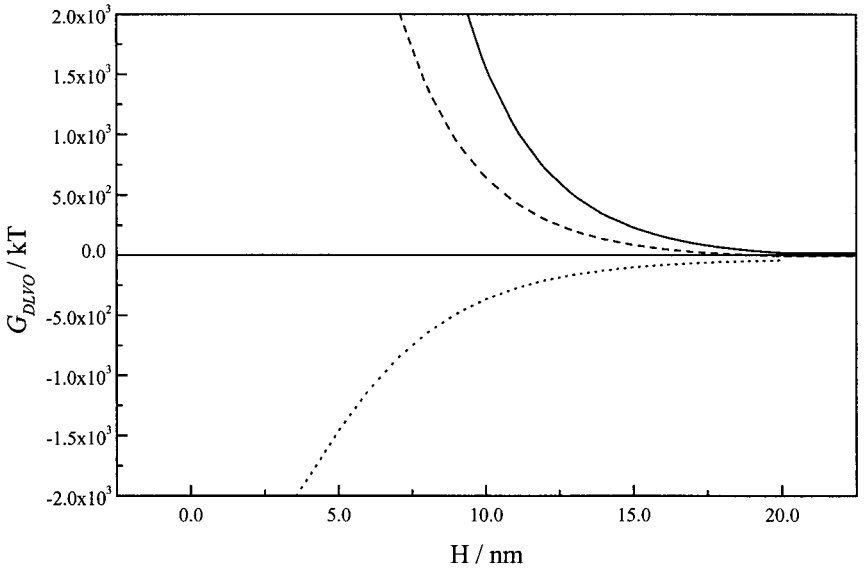

FIG. 4. DLVO interaction energy $G_{DLVO}(h)$ curves for bacterial cells and gold as a function of separation distance (H) at various surface potentials in 0.01 M NaCl. —, −0.57 V; – – –, −0.27 V; ·····, 0.13 V. The Hamaker constants for the gold surface, the bacterial surface, and the surrounding water were 62.5 kT (1), 15.3 $\boldsymbol{kT}$ (17), and 9.34 kT (17), respectively. The zeta potential for the bacterial surface was −0.0315 V.

15.3 kT (17), and 9.34 kT (17) were used for the Hamaker constants of the gold surface, the bacterial surfaces, and the surrounding water, respectively. The surface potential for bacterial cells was approximated to the value of their electrokinetic or zeta potential (ζ) (21). The values of ζ used in the calculations were −0.0315 and −0.0155 V at 0.01 and 0.1 M NaCl, respectively. These values were obtained from the electrophoretic migration (μ) measured values, as ζ equals 12.87 μ (5).

To determine the effective electrical potential value of the gold surface (ϕ_g) during the experiments, it was necessary to take into account the PZC of the metal surface. Values ranging from 0.00 to 0.07 V (Ag/AgCl-KCl sat.) were found in the literature (20). The ϕ_g values used in the DLVO calculations were −0.57, −0.27, and 0.13 V, when modeling the system at the surface experimental potentials of −0.5 V, −0.2 V, and E_{oc} (Ag/AgCl-KCl sat.), respectively.

The calculated interaction energy between gold and bacteria in 0.01 M NaCl at various surface potentials as a function of separation distance (H) can be seen in Fig. 4. With the gold surface at its E_{oc} (0.13 V versus the PZC), the interaction energy was strongly attractive, ranging from −43 kT at a separation distance of 20 nm to a primary minimum deeper than −1,800 kT at distances of less than 4 nm. On the basis of these calculations, irreversible adhesion would be expected at this potential.

With the metallic surface at negative potentials of −0.27 V and −0.57 V (versus the PZC), positive values of interaction energy in the liquid reached up to 20 nm. Values higher than 100 kT at separation distances of 10 to 15 nm determined the existence of extremely high energy barriers against bacterial adhesion as a consequence of the electrostatic repulsion.

At a higher ionic strength (0.1 M NaCl), the electrostatic interactions were shielded at separation distances larger than ~5 nm (Fig. 5). Calculations with the gold surface at E_{oc} resulted again in a primary minimum, indicating the possibility of irreversible adhesion. Nevertheless, the energy values in the proximity of the surface (<10 nm), were significantly higher (less negative) than those calculated at low ionic strength (Fig. 4), as a consequence of the diminution of the electrostatic attraction.

Calculations with the gold surface at negative potentials yielded deep secondary minima of −82.9 and −94.9 kT at separation distances of 7 and 6 nm, respectively, when potentials of −0.57 and −0.27 V were used. The interaction was strongly repulsive at distances shorter than 5 nm from the surface at both potentials (Fig. 5).

Reversible adhesion of *P. fluorescens* (ATCC 17552) to polarized gold. Calculations of the interaction energy between bacteria and gold at a high ionic strength (0.1 M NaCl) determined the existence of secondary energy minima when the surface was negatively polarized (Fig. 5). These secondary minima have been associated with the occurrence of reversible adhesion (3, 12, 14). In addition, the reversible adhesion of a *Pseudomonas* sp. to negatively polarized metal surfaces has been previously demonstrated (2). Since the experimental setup allows the direct observation of the behavior of bacteria in the polarized metal-electrolyte interface, experiments were carried out to verify if reversible adhesion of bacteria to gold occurs at the various potential and ionic strength conditions previously used. New sets of experiments were carried out in the absence of flow.

At low ionic strength (0.01 M), adhesion was detected only with the surface at its E_{oc}, as in the experiments using flow (Fig. 2). Once the bacterial cells approached the surface and adhered, no movements were observed. The irreversibility of the adhesion was proven at the end of the experiments by flowing distilled water through the chamber. The number of detached bacteria determined by digital image analysis was

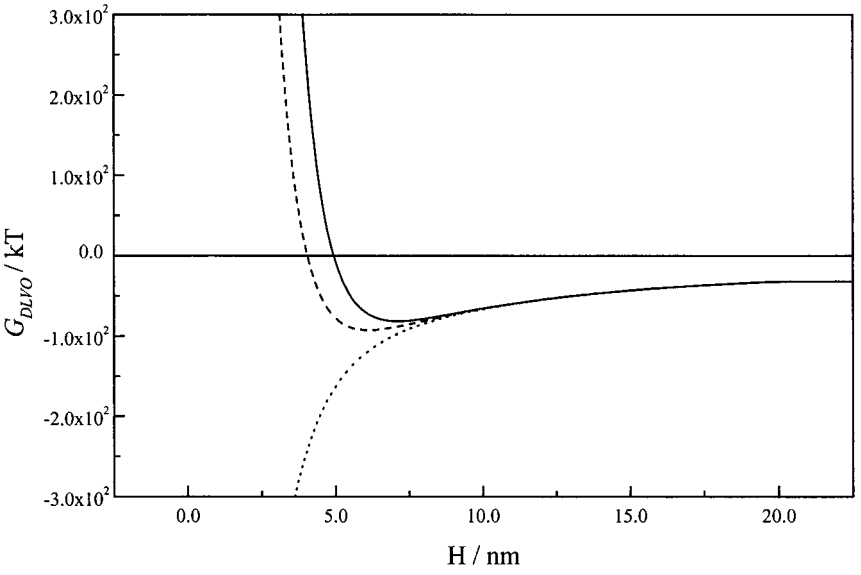

FIG. 5. DLVO interaction energy $G_{DLVO}(h)$ curves for bacterial cells and gold as a function of separation distance (H), at various surface potentials in 0.1 M NaCl. —, −0.57 V; – – –, −0.27 V; ·····, 0.13 V. The Hamaker constants for the gold surface, the bacterial surface, and the surrounding water were 62.5 kT (1), 15.3 kT (17), and 9.34 kT (17), respectively. The zeta potential for the bacterial surface was −0.0155 V.

zero, indicating that cells adhered irreversibly to the gold surface in these conditions.

At high ionic strength (0.1 M), different degrees of adhesion to the gold surface were detected at the various potentials (data not shown), resembling the results obtained using flow (Fig. 3). The adhesion to the surface at its E_{oc} was high and irreversible, as predicted by the DLVO interaction energy calculations (Fig. 5). On the other hand, the adhesion to the surface polarized to negative potentials (−0.5 and −0.2 V [Ag/AgCl-KCl sat.) was low, as shown in Fig. 3, but was also irreversible, in contrast to the presence of the secondary minima predicted by the DLVO calculations (Fig. 5). Although some bacterial cells described rotational movements during a few second fractions when attaching to the surface, no conclusive evidence for reversible adhesion was collected at these potentials.

To further investigate the occurrence of reversible adhesion, additional experimental determinations were made with the gold surface at a potential of 0.00 V (Ag/AgCl-KCl sat.), very close to the PZC potential of gold (20). Reversible adhesion was clearly observed at this potential. Video records were digitally decomposed, and sequential images were analyzed. The results shown in Fig. 6 showed that some bacteria moved rapidly in a plane parallel to the surface for a few seconds, describing a random walk in a clear association with the surface. During the translation, such bacteria occasionally sorbed at a pole, rotated in a propeller-like movement (Fig. 6), and then broke away. Some other bacteria just sorbed at a point and rotated before they broke away (Fig. 6). These kinds of movements have been described by other authors in previous papers (6, 12) in relation to the occurrence of reversible adhesion to glass. Irreversible adhered bacteria were also present during these experiments but were excluded from the results as a consequence of the differential character of the digital image analysis.

The observation of reversible adhesion was in good agreement with the existence of a deep secondary minimum of −133.1 kT located very close to the gold surface (4 nm) when a potential of −0.07 V (versus the PZC) was used, as shown by DLVO calculations (Fig. 7).

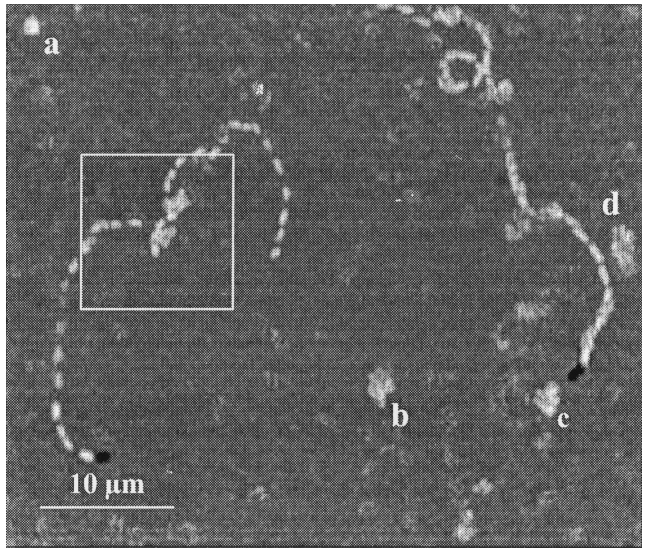

FIG. 6. Cumulative image showing reversible adhesion movements during polarization of gold to 0.00 V (Ag/AgCl-KCl sat.) in a bacterial suspension in 0.1 M NaCl. Sequential images were captured at a rate of 12 pictures s^{-1} during a 5-s interval. Each image was subtracted from the previous one, and the minimal gray value from every differential image was selected to construct the cumulative image. The box indicates the points where bacteria sorbed at the surface and broke away, during its translation movement. (a to d) Footprints indicating that a bacterial cell sorbed, rotated, and broke away during the sampling time.

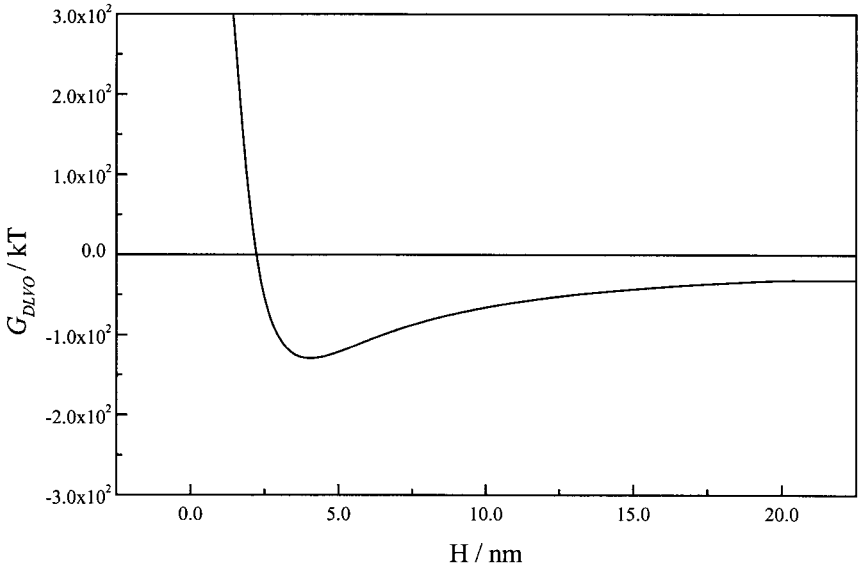

FIG. 7. DLVO interaction energy $G_{DLVO}(h)$ curves for bacterial cells and gold as a function of separation distance (H), at a surface potential of −0.07 V (versus the PZC) in 0.1 M NaCl. The Hamaker constants for the gold surface, the bacterial surface, and the surrounding water were 62.5 kT (1), 15.3 kT (17), and 9.34 kT (17), respectively. The zeta potential for the bacterial surface was −0.0155 V.

DISCUSSION

When a metal is immersed in an electrolyte solution, a potential difference is immediately established between them, with the formation of an electrical double layer. This double layer is composed by an excess of charge on the metal surface (σ_M), separated from an excess of the opposite charge on the solution side (σ_S) by a layer of adsorbed water molecules. The interfacial excess of charge on the solution side is a consequence of the accumulation of ions and is distributed towards the bulk solution forming a diffuse layer. The thickness of the diffuse layer (i.e., the protrusion of the charge to the bulk solution) is dependent on the solution ionic strength (18, 21). On the other side, the interfacial excess of charge on the metal surface is dependent on the surface electrochemical potential and can be modified externally by polarization. It follows that if the potential of the surface is shifted in the positive or negative direction, the charge σ_M increases in positive or negative value. The potential at which the interfacial charge is zero ($\sigma_M = -\sigma_S = 0$) is called the PZC (18).

Nonpolarized gold surfaces exhibit an open circuit potential of 0.2 ± 0.02 V (Ag/AgCl-KCl sat.) in NaCl solution, which is positive to the PZC of the material in the same electrolyte (0.00 − 0.07 V [Ag/AgCl-KCl sat.]) (20). The positive interfacial charge of the metal surface at this potential determines the electrostatic attraction against negatively charged bacteria, which, in addition to the van der Waals attraction forces, results in a deep primary minimum for the interaction energy, ranging from distances larger than 20 nm (Fig. 4 and 5). As predicted by the DLVO calculations shown in Fig. 4 and 5, the observed adhesion at this potential was irreversible under both ionic strength conditions and increased with the time of exposition. The number of adhered bacteria was higher at low ionic strength (Fig. 2) in accordance with the increased electrostatic attraction resulting from the decrease in shielding of the positive charge at the gold surface (Fig. 4). Since virtually all the cells which arrived at the surface adhered instantaneously, the rate of the adhesion process in these experiments was assumed to be dependent on the transport of cells to the surface.

Results shown in Fig. 2 and 3 indicated that bacterial adhesion to the gold surface can be significantly affected by polarization to negative potentials. The polarization to both, −0.5 and −0.2 V (Ag/AgCl-KCl sat.), imposed a strong negative charge to the metal surface, which resulted in a repulsive electrostatic interaction with the negatively charged bacterial cells. As was shown by the DLVO calculations, at low ionic strength (0.01 M NaCl) the electrostatic repulsion was increased (Fig. 4), protruding beyond 20 and 15 nm into the bulk solution at surface potential values of −0.57 and −0.27 V (versus the PZC), respectively. This should be the reason why the number of adhered bacteria to gold surfaces polarized to these potentials was strongly reduced (Fig. 2).

The thickness of the interfacial double layer and, in consequence, the influence of the electrostatic repulsion on the bacterial adhesion process are dependent on the ionic strength. When ionic strength was increased to 0.1 M NaCl, the interaction energy between negatively polarized gold electrodes and bacteria was found to be repulsive at shorter distances and became attractive at distances larger than ~5 nm (Fig. 5). The shielding of electrostatic repulsion can explain the slightly increased bacterial adhesion at high ionic strength observed at a potential of −0.2 V (Fig. 3), in relation to the one observed at the low ionic concentration at the same potential (Fig. 2). At a more-negative potential (−0.5 V), however, the adhesion remained very low (Fig. 3), probably due to the higher levels of interaction energy at critical distances of 4 to 5 nm.

The overall interaction energy in 0.1 M NaCl (Fig. 5) presented relatively deep secondary minima at 7 and 6 nm from the gold surface, when potentials of −0.57 and −0.27 V, respectively (versus PZC) were used. In spite of the presence of these minima very close to the surface, the observed adhesion

was irreversible, and no evidences of reversible adhesion could be collected when experiments were carried out at these negative potentials in the absence of flow.

The discrepancy between experimental and calculated results could be related to the participation of specific interactions (3). Also, the gold surface could be conditioned as a consequence of the adsorption of excreted metabolites, and surface properties could be slightly altered. However, the constancy of adhesion slopes shown in Fig. 2 and 3 indicates that conditioning of the initially clean surface does not occur during the experiments or does so at a minor rate.

Regarding specific interactions, it was proposed that bacteria adhere to the surface of minerals (10) and metal oxides (J. P. Busalmen and S. R. de Sánchez, submitted for publication) through the formation of hydrogen bonds. Gold surfaces support covalent bonding with water molecules in the molecular state in order to compensate for the excess of surface charge. Since the energy of these covalent bonds is close to the energy of hydrogen bonds, adsorbed water molecules are combined not only with the metal surface but also with water and other molecules by hydrogen bonding (18). The excess of surface charge on a metal surface gradually disappears with the formation of succeeding layers of water molecules. On the other side, it was emphasized that DLVO interactions of bacterial cells more likely originate from a deeper shell in the cell core, other than at the cell surface, and that the projection of a few lipopolysaccharide molecules could anchor the cell irreversibly to the surface (9).

The width of a water layer is about 0.25 nm, and the formation of several layers at surface potentials where the surface charge density is high (far from the PZC) could bridge the distance to the bacterial cells at the secondary minimum, allowing the formation of hydrogen bonds with the lipopolysaccharide on the bacterial surface and yielding irreversible adhesion in spite of energy barriers.

The absence of reversibly adhered bacteria could be related to both phenomena: the quick change to irreversible adhesion through the formation of hydrogen bonds as soon as bacteria reached the secondary minimum and the electrophoretic migration of negatively charged bacteria far from the gold surface along the electric field generated in a direction perpendicular to the surface, as a consequence of the potential difference between the WE and the CE.

Reversible adhesion was observed only when the gold surface was polarized to a potential very close to its PZC (0.00 V [Ag/AgCl-KCl sat.]). Due to the low overpotential, the surface charge was very low and the electrostatic repulsion was reduced to distances shorter than ~2.5 nm (Fig. 7). In contrast to the situation on a strongly polarized surface, neither the organization of water layers nor the presence of an electric field is significant enough to interfere with the presence of bacteria reversibly sorbed at the secondary minimum. In addition, the depth of the secondary minimum was enough to retain bacteria very close to the surface (4 nm) but allow movements in the parallel plane as shown in Fig. 6.

ACKNOWLEDGMENTS

The present research was supported by a grant (PIP 4339) from CONICET-Argentina.

Useful discussions with A. Regazzoni are gratefully acknowledged.

REFERENCES

1. **Biggs, S., and P. Mulvaney.** 1994. Measurement of the forces between gold surfaces in water by AFM. J. Chem. Phys. **100:**8501–8505.
2. **Busalmen, J. P., S. R. de Sánchez, and D. J. Schiffrin.** 1998. Ellipsometric measurement of bacterial films at metal-electrolyte interfaces. Appl. Environ. Microbiol. **64:**3690–3697.
3. **Busscher, H. J., and A. H. Weerkamp.** 1987. Specific and non-specific interactions in bacterial adhesion to solid substrata. FEMS Microbiol. Rev. **46:** 165–173.
4. **de Sánchez, S. R., and D. J. Schiffrin.** 1985. The effect of pollutants and bacterial microfouling on the corrosion of copper base alloys in seawater. Corrosion **41:**31–38.
5. **Einolf, C. W., and E. L. Carstensen.** 1967. Bacterial conductivity in the determination of surface charge by electrophoresis. Biochim. Biophys. Acta **148:**506–516.
6. **Frymier, P. D., R. S. Ford, H. C. Berg, and P. T. Cummings.** 1995. Three-dimensional tracking of motile bacteria near a solid planar surface. Proc. Natl. Acad. Sci. USA **92:**6195–6199.
7. **Gristina, A. G.** 1987. Biomaterial-centered infection: microbial adhesion versus tissue integration. Science **237:**1588–1595.
8. **Jucker, B. A., H. Harms, and A. J. B. Zehnder.** 1996. Adhesion of the positively charged bacterium *Stenotrophomonas* (*Xanthomonas*) *maltophilia* 70401 to glass and Teflon. J. Bacteriol. **178:**5472–5479.
9. **Jucker, B. A., H. Harms, and A. J. B. Zehnder.** 1998. Polymer interactions between five gram-negative bacteria and glass investigated using LPS micelles and vesicles as model systems. Colloids Surf. B Biointerfaces **11:**33–45.
10. **Jucker, B. A., H. Harms, S. J. Hug, and A. J. B. Zehnder.** 1997. Adsorption of bacterial surface polysaccharides on mineral oxides is mediated by hydrogen bonds. Colloids Surf. B Biointerfaces **9:**331–343.
11. **Marshall, K. C.** 1994. Microbial adhesion in biotechnological processes. Curr. Opin. Biotechnol. **5:**296–301.
12. **Marshall, K. C., R. Stout, and R. Mitchell.** 1971. Mechanism of the initial events in the sorption of marine bacteria to surfaces. J. Gen. Microbiol. **68:**337–348.
13. **Meinders, J. M., H. C. van der Mei, and H. J. Busscher.** 1992. In situ enumeration of bacterial adhesion in a parallel plate flow chamber—elimination of in focus flowing bacteria from the analysis. J. Microbiol. Methods **16:**119–124.
14. **Norde, W., and J. Lyklema.** 1989. Protein adsorption and bacterial adhesion to solid surfaces: a colloid-chemical approach. Colloids Surf. **38:**1–13.
15. **Pitt, W. G., M. O. McBride, A. J. Barton, and R. D. Sagers.** 1993. Air-water interface displaced adsorbed bacteria. Biomaterials **14:**605–608.
16. **Rijnaarts, H. H. M., W. Norde, E. J. Bouwer, J. Lyklema, and A. J. B. Zehnder.** 1993. Bacterial adhesion under static and dynamic conditions. Appl. Environ. Microbiol. **59:**3255–3265.
17. **Rijnaarts, H. H. M., W. Norde, E. J. Bouwer, J. Lyklema, and A. J. B. Zehnder.** 1995. Reversibility and mechanism of bacterial adhesion. Colloids Surf. B Biointerfaces **4:**5–22.
18. **Sato, N. (ed.).** 1998. Electrochemistry at metal and semiconductor electrodes, p. 119–196. Elsevier Science, Amsterdam, The Netherlands.
19. **Shabtai, Y., and G. Fleminger.** 1994. Adsorption of *Rhodococcus* strain GIN-1 (NCIMB 40340) on titanium dioxide and coal fly ash particles. Appl. Environ. Microbiol. **60:**3079–3088.
20. **Sokolowski, J., J. M. Lzajkowski, and M. Turowska.** 1990. Zero charge potential measurements of solid electrodes by inversion immersion methods. Electrochim. Acta **35:**1393–1398.
21. **Stumm, W., and J. J. Morgan.** 1981. Aquatic chemistry, p. 599–682. J. Wiley & Sons, New York, N.Y.
22. **Wang, I., J. M. Anderson, M. R. Jacobs, and R. E. Marchant.** 1995. Adhesion of *Staphylococcus epidermidis* to biomedical polymers: contributions of surface thermodynamics and hemodynamic shear conditions. J. Biomed. Mater. Res. **29:**485–493.